Effect of different building materials on conjugate heat and mass transfer

M. Gijón-Rivera[a]*, J. Serrano-Arellano[b], J. Xamán[c], G. Álvarez[c]

[a]Tecnologico de Monterrey, Escuela de Ingeniería y Ciencias
Vía Atlixcáyotl 2301, Reserva Territorial Atlixcáyotl, Puebla, Puebla, C.P. 72453, México
miguel.gijon@itesm.mx

[b]División de Arquitectura e Ingeniería en Energías Renovables, Instituto Tecnológico Superior de Huichapan-ITESHU-TecNM
Dom. Conocido S/N, El Saucillo, Huichapan, Hidalgo, C.P. 42411, México
jserrano@iteshu.edu.mx

[c]Centro Nacional de Investigación y Desarrollo Tecnológico. CENIDET-TecNM
Prol. Av. Palmira S/N. Col. Palmira. Cuernavaca, Morelos, CP. 62490, México
jxaman@cenidet.edu.mx , gaby@cenidet.edu.mx

Resumen

En este artículo se presenta un estudio numérico del efecto de la conducción de calor de diferentes materiales de construcción sobre la transferencia de calor y masa en una cavidad rectangular. El aire al interior de la cavidad se encuentra contaminado con CO_2. Las ecuaciones de conservación de masa, momentum, energía, especies y el modelo de turbulencia k-ε fueron resueltas usando la técnica de volumen finito. El caso A (bloque de adobe) fue la configuración óptima desde el punto de vista del confort térmico. En general, el caso B (ladrillo rojo) fue la mejor opción desde el punto de vista de la calidad del aire interior con una diferencia de 200 ppm con respecto a otros materiales de construcción y para todos los números de Rayleigh analizados.

Abstract

A numerical analysis of the effect of heat conduction of different building materials on conjugate heat and mass transfer in a square cavity is presented. The air fluid inside the cavity is contaminated with Carbon Dioxide (CO_2). The governing equations of mass, momentum, energy and concentration with a turbulent k-ε model were solved by the finite-volume technique. From the thermal point of view, case A (adobe block) was the optimal configuration in order to reach comfortable conditions. In general, the case B (red brick) was the best choice for air quality purposes with a difference of 200 ppm with respect to other building materials for all Rayleigh numbers under study.

Palabras clave:

Conducción de calor, convección natural turbulenta, transferencia de masa, radiación térmica superficial, cavidad cuadrada

Keywords:

Heat conduction, turbulent natural convection, mass transfer, surface thermal radiation, square cavity

List of Symbols

C	concentration of the pollutant or chemical species, Kg/m³ ó ppm.
Cp	specific heat, J/Kg K.
dF_{j-k}	view factor between elements j-k.
G	normal solar radiation, W/m².
Hx	cavity width, m.
Hy	cavity height, m.
Hw	conductive wall width, m.
Nu	average Nusselt number, $Nu=q_{conv}/q_{ref}$
P	fluid pressure, N/m².
q	heat flux, (W/m²)
S_g	extinction coefficient (m⁻¹)
Ra	Rayleigh number, $Ra=g\beta(T_{wall}-T_C)L^3/\upsilon\alpha$.
$S\varphi$	source term.
T	temperature, ºC ó K.

T_{ave}	$T_{ave}=\int^n\left[\dfrac{T_i}{n}\right]dxdy$
u	speed in the horizontal direction, m/s.
v	speed in the vertical direction, m/s.
x, y	coordinate x, y.

Greek

Γ	diffusion coefficient.
ε	emissivity.
λ	thermal conductivity of the fluid, W/m K.
ρ^*	reflectivity.
ρ	density of the mixture, kg/m³.
σ	Stefan-Boltzmann constant (5.67×10^8 W/m² K⁴).
τ	Transmissivity.
ϕ	dependent general variable (u, v, P, T).

EDICIÓN DIGITAL

Subscripts

C	cold
cond	conductive
conv	convective
H	hot
i	Interior
o	exterior
rad	radiative
tot	total

Introduction

Conjugate heat transfer studies in closed cavities have many engineering applications, such as solar collectors, nuclear reactors, cooling of electronic systems, building design applications, etc. In particular, theoretical research in building thermal design provides the opportunity to quantify the heat transfer in complex systems in order to obtain thermal parameters required in commercial software or for making decisions at different building design stages. Also, it is well known that the interaction between indoor spaces and the environment is highly influenced by the type of building materials (thermophysical and optical properties): opaque and/or semitransparent walls. Thermal energy gains or losses through the envelope directly affect the thermal comfort of occupants and the final energy consumption inside rooms. On the other hand, building occupants are the main source of CO_2 emissions inside rooms, making mandatory the analysis of coupling heat and mass transfer in order to satisfy indoor air quality standards. Therefore, conjugate natural convection with surface radiation, mass transfer and conducting walls in closed cavities are worthy of research. A short literature review is presented next. For example, in 1976 Larson and Viskanta [1] reported a numerical study of conjugate heat transfer in a square cavity with opaque and diffusive walls. The authors found that thermal radiation is dominant. Weeb and Viskanta [2] included the heat condition through a semitransparent wall, showing that 70% of the energy incoming to the cavity was provided by direct absorption of thermal radiation. Later, Behnia et al. [3] analysed a closed cavity with a semitransparent wall considering convective losses to the surroundings. They studied the effect of external convection and surface thermal radiation on heat transfer inside the cavity. Kwon et al. [4] reported the effect of considering a glazed surface in the middle of vertical conductive wall in the closed cavity. More recently, Álvarez and Estrada [5] considered a semitransparent wall with a solar film adhered to the inside surface. They found that total energy transferred to the air through the glass wall with a control film is lower than the case of the simple clear glass. Zhao et al. [6] investigated the fluid flow and heat transfer in square enclosures representing building elements. They evaluated conjugated heat conduction and natural convection in laminar flow regime. Results reveled that heat transfer rates across both enclosures are complex functions of the volume ratio scale, Rayleigh number, and the relative thermal conductivity. Xamán et al. [7-10] reported several studies of conjugate heat transfer in closed cavities with conducting walls in laminar and turbulent flow regimes. They have analysed the effect of solar control coatings on heat transfer, surface thermal radiation contribution, and the effect of different roof materials on thermal comfort inside cavities with real room sizes. In the same way, Kuznetsov and Sheremet [11-18] published several works of conjugate heat transfer in enclosures with finite thickness heat-conducting walls at different physical conditions. For example, they reported the effect of local heat sources at different positions, heat transfer problems with internal mass transfer, the analysis of convective and radiative heat exchange with the environment on particular wall surfaces, numerical investigations at different flow regimes (laminar and turbulent), analysis of steady or unsteady conditions, two or three dimensional enclosures and, finally the contribution of temperature and concentration gradients on heat and mass transfer (double diffusive phenomena). Gijón-Rivera et al. [19] presented a numerical simulation for a room on top a building considering natural convection and surface thermal radiation with opaque and semitransparent walls interacting with surroundings by convection and radiation. Authors reported a sensitive analysis of the effect of windows and the coupled-decoupled solutions on indoor air temperatures and thermal loads inside rooms. Finally, Serrano-Arellano and Gijón-Rivera [20] reported a numerical solution of conjugate heat (convection-radiation) and mass transfer in a square cavity filled with a mixture of Air-CO_2. They found that convection increases as the mass transfer is taking into account but decreases as the Rayleigh number increases.

As it is observed in the state of art, there are only few studies of conjugate heat transfer (turbulent convection, radiation and conduction) inside enclosures due to its complexity. Thus, we can say that there has not been found a conjugate heat transfer study with a conducting wall in a closed cavity filled with a contaminated fluid (Air-CO_2) in turbulent flow regime. The purpose of the present work is to analyse the effect of heat conduction of different conductive walls on conjugate heat and mass transfer by turbulent natural convection of a room modeled as a square cavity. Four different building materials typically used in Latin-American countries (warm climates), such as Mexico and Peru are selected as the conductive wall configurations: red brick, clear glass, concrete block and adobe block. Statistical information shows that 14.6% of Mexican houses are built of adobe walls, followed by 69.5% made of red brick [21]. Otherwise, government information from Peru shows that the most common wall material used to build houses is the red brick or concrete block with 51.5%, followed by the adobe block with 34.1% [22]. Adobe is a construction material formed by a mixture of straw and mud used since pre-Hispanic age and typically used for building rustic houses. Nowadays the adobe block is deeply used in medium and high-income houses in Mexico.

Marzo 2016, Vol. 5

396 Gijón-Rivera M., Serrano-Arellano J., Xamán J., Álvarez G.

Physical and Mathematical Models

A two-dimensional closed cavity filled with a mixture of Air-CO_2 is shown in Fig.1. The working fluid is initially considered to be at rest with a uniformly distributed temperature and concentration inside the cavity. The square cavity can be assumed to be of infinite depth along z axis. The left vertical surface of the cavity is considered to be an isothermal opaque wall at 25°C (TC) with a CO_2 concentration of 500 ppm (CC) The horizontal top and bottom wall are considered adiabatic and impermeable. The right vertical surface is considered as a conductive wall with three different building materials (opaque and semitransparent): case A (adobe block), case B (red brick), case C (concrete block) and case D (single clear glass); this vertical surface is kept at a higher CO_2 concentration of 3000 ppm (CH). On the vertical conductive surface an incoming normal uniform and constant solar radiation flux of 736 W/m² (AM2) was considered and two dimensional heat transfer by conduction is taken into account. Furthermore, in the conductive wall take place a temperature difference between external surface and the environment allowing the presence of convective and radiative heat fluxes to the exterior. In the case of the semitransparent surface, part of the energy is reflected, part is transmitted through and part is absorbed by the wall, whereas in the case of the opaque surface the radiative energy transmitted through it is not considered. The semitransparent and opaque walls of the cavity were considered gray, diffusive, reflective, and radiation emitter surfaces. The thermal fluid was considered steady, radioactively non-participating. The Boussinesq approximation is assumed with constant thermophysical and optical properties are the integrated spectrum values. Finally, thermophysical properties were calculated by using the methodology reported by Reid et al. [23].
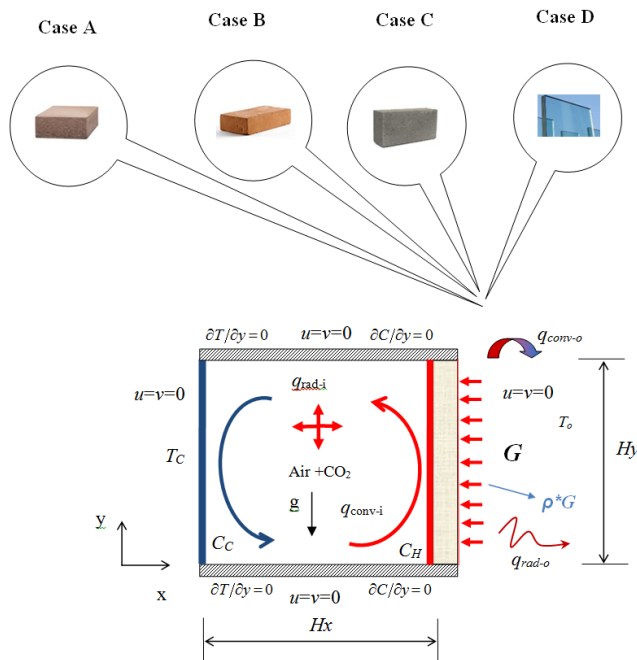

Fig. 1 Physical model for the square cavity with a conductive wall.

Convective mathematical model

The convective mathematical model is formulated taking into account several assumptions such as: non-slip condition at walls is valid. Any chemical reaction and heat generation/dissipation inside the enclosure is not considered. The energy flux produced by mass transfer (Dufour effect) and the mass flux produced by the energy transfer (Soret effect) are not considered. The contaminant is considered at lower density than the air (raising motion). The working fluid is considered as a Newtonian fluid in steady state. The governing equations for turbulent natural convection in a square cavity are the average equations of mass, momentum, energy and species presented below:

$$\frac{\partial(\rho u_i)}{\partial x_i} = 0 \tag{1}$$

$$\frac{\partial(\rho u_i u_j)}{\partial x_j} = -\frac{\partial P}{\partial x_i} + \frac{\partial}{\partial x_j}\left[\mu\left(\frac{\partial u_i}{\partial x_j} + \frac{\partial u_j}{\partial x_i}\right) - \rho\overline{u_i' u_j'}\right] +$$
$$+ \rho g_i \beta(T - T_\infty) + \rho g_i \beta_C(C - C_\infty) \tag{2}$$

$$\frac{\partial(\rho u_j T)}{\partial x_j} = \frac{1}{Cp}\frac{\partial}{\partial x_j}\left(\lambda\frac{\partial T}{\partial x_j} - \rho Cp\overline{u_i' T'}\right) \tag{3}$$

$$\frac{\partial(\rho u_j C)}{\partial x_j} = \frac{\partial}{\partial x_j}\left(\rho D_{AB}\frac{\partial C}{\partial x_j} - \rho\overline{u_i' C'}\right) \tag{4}$$

In order to close the turbulence mathematical problem, the turbulent kinetic energy ( ) and the turbulent kinetic energy dissipation ( ) are required:

$$\frac{\partial(\rho u_i k)}{\partial x_i} = \frac{\partial}{\partial x_i}\left[\left(\mu + \frac{\mu_t}{\sigma_k}\right)\frac{\partial k}{\partial x_i}\right] + P_k + G_k - \rho\varepsilon \tag{5}$$

$$\frac{\partial(\rho u_i \varepsilon)}{\partial x_i} = \frac{\partial}{\partial x_i}\left[\left(\mu + \frac{\mu_t}{\sigma_\varepsilon}\right)\frac{\partial\varepsilon}{\partial x_i}\right] + C_{\varepsilon1}\left[P_k + C_{\varepsilon3}G_k\right]\frac{\varepsilon}{k} - C_{\varepsilon2}\frac{\rho\varepsilon^2}{k} \tag{6}$$

The k-ε turbulence model defines the following variables $C_{\varepsilon1}$=1.44, $C_{\varepsilon2}$=1.92, $C_{\varepsilon3}$=$tan\ h|v/u|$, C_μ=0.09, σ_k=1.0 and σ_ε=1.3 (HH model proposed by Henkes *et al*, [24]).

The boundary conditions of the mathematical convective model for the hydrodynamic, thermal and mass transport are as follows:

The velocity boundary conditions at solid surfaces are:

u=v=0

The thermal and mass boundary conditions are:

$\partial T/\partial y + qrad$=0 and $\partial C/\partial y$=0, at y = 0 and y =Hy

$T=T_C$ and $C=C_C$, at x = 0

$\lambda(\partial T/\partial y)+q_{rad}=\lambda_{wall}(\partial T/\partial y)$ and $C=C_{HP}$, at x =Hx

Heat conduction mathematical model

Fig. 2 shows the physical model of the conductive surface interacting with external and internal conditions. In order to calculate the energy transferred through the wall the conductive model is dominated by the differential heat conduction equation given by:

$$\frac{\partial}{\partial x_j}\left(\frac{\lambda_{wall}}{Cp_{wall}}\frac{\partial T_{wall}}{\partial x_j}\right)+\frac{1}{Cp_{wall}}\frac{\partial \Theta}{\partial x}=0 \tag{7}$$

where λ_{wall} is the thermal conductivity, T_{wall} is the temperature, Cp_{wall} is the specific heat of the wall and Θ is the energy attenuation function by absorption and scattering, which depends on the extinction coefficient (S_g) as $\Theta(x)=G\exp(-S_g(Hw-x))$, not considered for opaque walls [25].
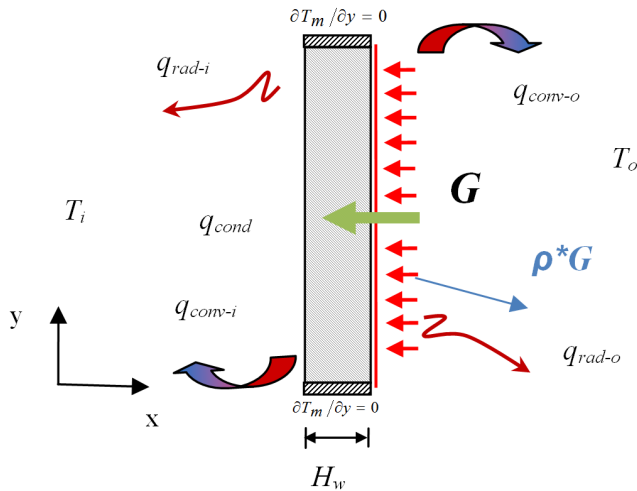

Fig 2. Physical model of the conductive right wall.

The wall thicknesses is considered as 6 mm for the semitransparent surface and 120 mm for the opaque surfaces under study. Thermal boundary conditions in the conductive surface are: adiabatic at lower ($y = 0$) and upper ($y = H_y$) surfaces, that is $\partial T_{wall}/\partial y$ =0; in the zone in contact with the environment, a constant heat flux is imposed with convective and radiative losses to the ambient with a temperature T_o, that is to say, $q_{cond\text{-}wall}+\alpha\cdot G=q_{conv\text{-}0}+q_{rad\text{-}0}$($x = H_x+H_{wall}$). In order to obtain the internal wall temperature distribution To, the following energy balance was conducted ($x = Hx$): $q_{cond\text{-}wall}=q_{conv\text{-}i}+q_{rad\text{-}i}$. Lastly, thermophysical and optical properties of the different conductive walls are shown in Table 1.

Surface thermal radiation model

The internal radiative exchange among surfaces was carried out by mean of the net radiation method described by Siegel and Howell [26]. All inner surfaces are considered to be opaque and diffuse except for the case of the semitransparent surface. The heat transfer by radiation from a surface is defi-

Marzo 2016, Vol. 5

398 Gijón-Rivera M., Serrano-Arellano J., Xamán J., Álvarez G.

ned as the difference between the outgoing radiative energy (radiosty) and the incoming radiative energy (irradiance). The radiative heat flux for the j_{th} element on each wall is given by the following energy balance:

$$q_{r_j}\left(x_j\right)=q_{o_j}\left(x_j\right)-q_{i_j}\left(x_j\right) \tag{8}$$

Table 1. Thermophysical and optical properties of the conductive wall.

Material	ρ (kg/m³)	λ (W/m K)	C_p (J/kgK)	ε	α	ρ^*	τ
Adobe Block	1620	0.49	1240	0.90	0.85	0.15	0
Red Brick	1800	0.72	829	0.90	0.93	0.07	0
Concrete Block	2300	1.4	880	0.90	0.65	0.35	0
Clear Glass	2500	1.4	750	0.85	0.14	0.08	0.78

where the radiosity for the jth element is defined as:

$$q_{o_j}\left(x_j\right)=\varepsilon_j^*\sigma T_j^4\left(x_j\right)-\rho_j^*q_{i_j}\left(x_j\right) \tag{9}$$

the irradiation is given by:

$$q_{i_j}\left(x_j\right)=\sum_{k=1}^{m}\int_{A_k}q_{o_j}\left(x_k\right)dF_{dA_j-dA_k} \tag{10}$$

where the summation over the k_{th} surface element is to be taken for those elements over the boundary for which j interacts radiatively and dF$_{j\text{-}k}$ is the differentially view factor, which is calculated using the crossed string method for the two-dimensional square cavity.

Numerical solution and verification

The set of transport differential equations are mathematically replaced by the general discretized in tensorial form as:

$$\frac{\partial}{\partial x_j}\left(\rho u_j\phi\right)=\frac{\partial}{\partial x_j}\left(\Gamma\frac{\partial \phi}{\partial x_j}\right)+S_\phi \tag{11}$$

The generalized equation described above can be expressed as every particular transport equation where, ρ is the density of the mixture of fluid (kg/m³), u_j is the velocity component (m/s), ϕ is the general transport variable, Γ is the diffusion coefficient and S_ϕ is the source term. Once the mathematical model has been established, the spatial derivatives are discretized using the finite volume method suggested by Patankar [27] on a non-uniform staggered grid. The general convection-diffusion equation (1) is integrated on a control volume, obtaining an algebraic equation for each nodal point as:

$$a_p\phi_p^{n+1}=\sum_{nb}a_{nb}\phi_{nn}^{n+1}+S_\phi\Delta V+\rho^n\Delta V\phi_p^n \tag{12}$$

From the above equation n y nb represent the number of iterations and the coefficients for the neighborhood nodes, respectively; b is the source term, and ϕ is the discrete dependent variable over each control volume. The convective terms are approximated by the power law scheme and diffu-

sive terms by the central scheme. The false transient approach is used to increase the convergence of the numerical algorithm. The coupling between the mass and momentum equations is made with the SIMPLEC algorithm proposed by Van Doormal and Raithby [28]. The algebraic equations system is solved with the line by line method (LBL) with alternating direction implicit scheme (ADI). The solution converges when mass balance residuals are at least 10-8. A radiative balance over walls is iteratively treated in order to obtain net energy fluxes by radiation needed by the conjugate heat transfer model. The radiosity equations were solved by the Simpson´s rule and the view factors between the elements were obtained by the Hottel´s cross string method proposed by Modest [25].

The accuracy of the numerical results was verified through numerous tests based on the grid size effect. It was found an adequate mesh for 101×101 with non-significant differences for the velocity, temperature, concentration and for all the Rayleigh numbers under study. The numerical code developed in FORTRAN programing language have been deeply verified and validated using different problems from literature such as: (a) laminar natural convection and mass transfer in a differentially heated square cavity [29]; (b) the benchmark solution of natural convection with turbulent flow in a square cavity [30]; (c) the experimental results of the natural convection in turbulent flow regime in an air filled square cavity [31]; and, (d) the natural convection analysis with radiation in a differentially heated square cavity [32]. All these comparisons have been reported on diverse previous publications [19, 20]; from these comparison results and their good agreement, we considered our code sufficiently tested.

Results and discussion

The parameters of the study used to obtain the conjugate heat and mass transfer for the square cavity with conductive walls are describe next. The size of the cavity was varied from 0.5 to 2.0 m, which correspond to $2.56 \times 10^9 \leq Ra \leq 1.63 \times 1011$. The solar radiation is considered as incident in normal direction on the conductive wall with a constant value of 736 W/m² (AM2). The opaque wall has the thickness of a typical building block of 120 mm and the semitransparent wall thickness considered was 6 mm as a single clear glass sheet. Temperature on the isothermal wall (Tcold) is 25°C with a low CO_2 concentration of 500 ppm (CL); whereas the conductive vertical wall was kept at a high CO_2 concentration of 3000 ppm (CH). The external conditions existing over the conductive wall were: a heat transfer coefficient of 6.8 W/m²K (3 m/s) and an outdoor temperature of 308 K. A parametric study to evaluate the effect of the opaque and semitransparent wall on heat and mass transfer was performed taking into account the next building materials: case A (block adobe), case B (red brick), case C (block concrete) and case D (single clear glass).

Flow patterns inside the cavity (streamlines, isothermals and isoconcentrations)

The streamlines, isothermals and isoconcentration distribution for the different building materials in the conductive wall and for the interval of the Rayleigh number considered in this study are showed below. Streamlines contours for all cases of study are graphically presented in Fig. 3. As can be seen, a counterclockwise recirculating flow pattern inside the cavity is observed due to energy delivered by the conductive
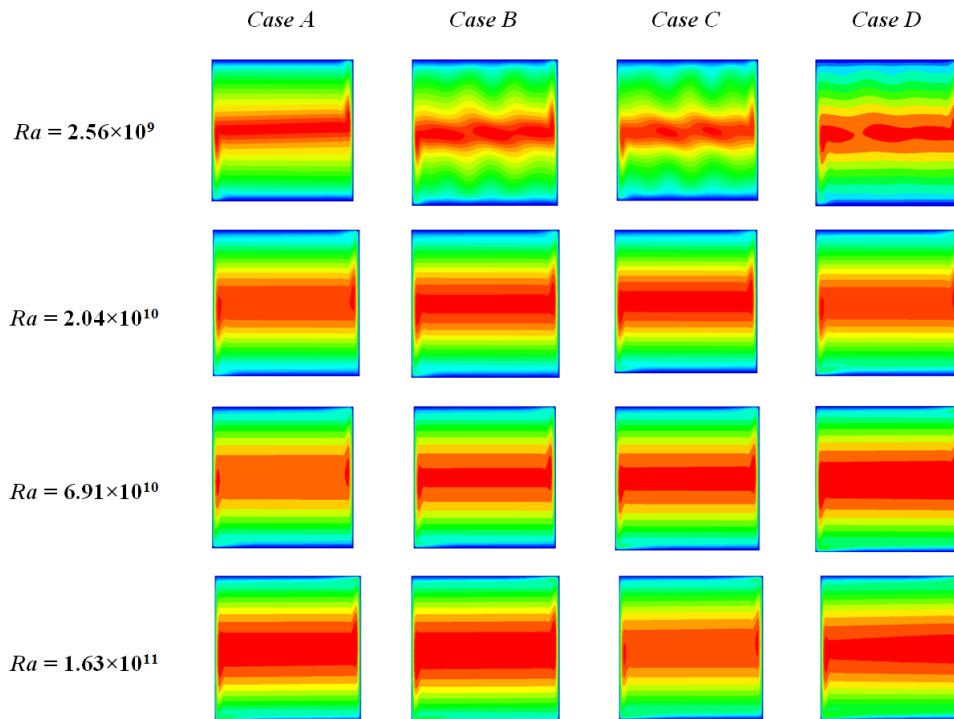

Fig. 3 Streamlines contours for all Ra numbers analysed: Case A (adobe block), Case B (red brick), Case C (concrete block) and Case D (single glass), from left to right, respectively.

wall and buoyancy forces acting upon the fluid for all cases under study. It can be note that most marked differences in fluid motion are especially presented at lower *Ra* numbers. In particular, the case D for $Ra = 2.56 \times 10^9$ shows a core recirculation divided into two central zones, which produces a non-symmetrical flow distribution inside the cavity with slight flow fluctuations. As the *Ra* number increases, a symmetric behavior of the flow with regard to the centre of the cavity is observed. The fluid motion is concentrated in the zone near walls owing to high velocity gradients located in the boundary layer region (the fluid is confined at the centre of the space); this faster movement of fluid next to the boundaries is also an indication of higher levels of turbulence. For high values of Rayleigh ($Ra \geq 2.04 \times 10^{10}$), at the centre of the cavity a main recirculation is formed, causing an important fluid stratification in the upper and bottom sides of the cavity for all wall materials.

Fig. 4 shows the isotherms patterns inside the cavity for all cases analysed. The thermal energy supplied from the vertical conductive wall of the cavity causes an upward movement of fluid until reaching the top of the cavity and towards the isothermal wall. In this zone, the fluid loses energy starting a descending movement in the direction of the bottom wall. At that time, a new rotation starts once again for finally reaching the thermal equilibrium. It can be observed that high horizontal thermal stratification occurs in most of the cavity for all *Ra* numbers. As the *Ra* number increases, the isotherms at the centre of the cavity are quasi-horizontal, becoming vertical over the boundary layer region and forming stratified multilayers throughout the cavity.

As expected, the case D shows higher fluid temperatures inside the cavity due the nature of the semitransparent wall. However, an important finding was that the case A presents lower temperatures inside the cavity among cases. The cavity with wall made of adobe has temperature differences between 2 to 4°C compared to the case B and between 4 to 6°C with respect to the case C configuration. In general, as the Ra number increases, the fluid temperature in the bottom side of the cavity increases, remaining almost constant in the rest of the cavity, especially for the case of opaque walls. In addition, the lowest temperature differential (ΔT) is observed for the case A, which indicates that it has a more thermally homogeneous space inside the cavity. Finally, it can be seen how the stratification drastically diminishes from $Ra = 6.91 \times 10^{10}$ for the case D configuration; the cavity is divided into two big zones with uniform temperatures, covering approximately the 90% of the space. This thermal behavior is clearly different to those found in previous studies, such as [7], which can be attributed to the mixture of Air-CO_2 considered inside the cavity (combined effect of conjugate heat and mass transfer).

Fig. 5 shows the isococentration behavior at the inside of the cavity. In general, it can be noted that the CO_2 concentration differential (ΔC) decreases as the *Ra* number increases from 1400 to 400 ppm for all cases considered in this study. Also, it can be seen that there exists a small influence of wall materials on CO_2 concentration for all Ra numbers. However, it can be observed that the case B shows the lowest concentration levels with less than 200 ppm for all *Ra* numbers and among building materials. In general, case B can be adopted as an optimal configuration from the air quality standpoint.
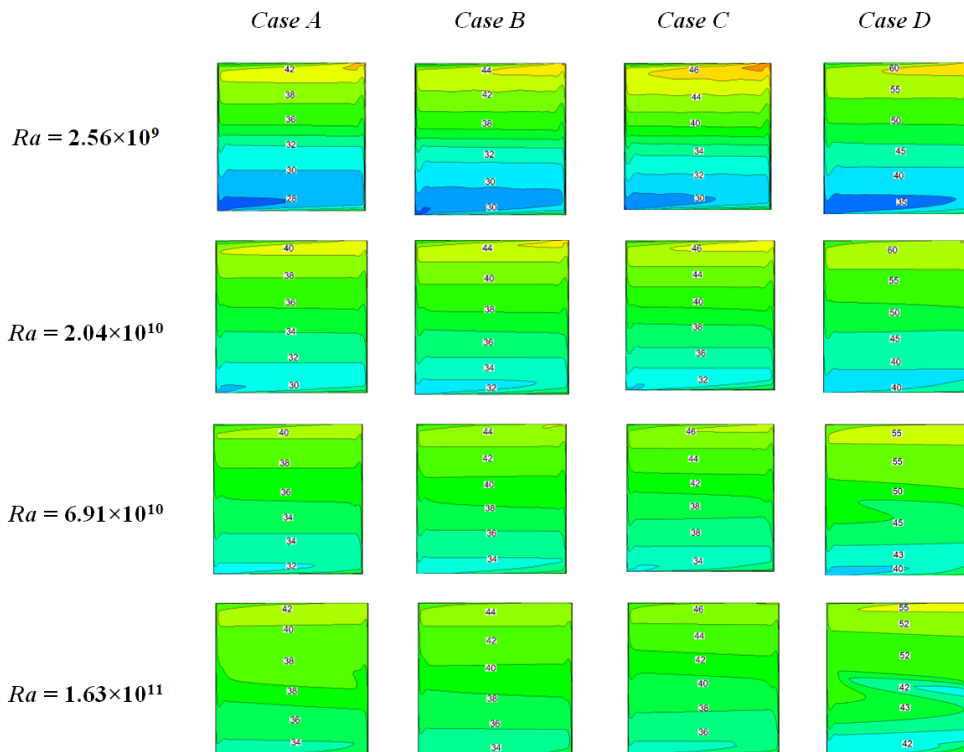

Fig. 4 Isotherms for all Ra numbers analysed: Case A (adobe block), Case B (red brick), Case C (concrete block) and Case D (single glass), from left to right, respectively.
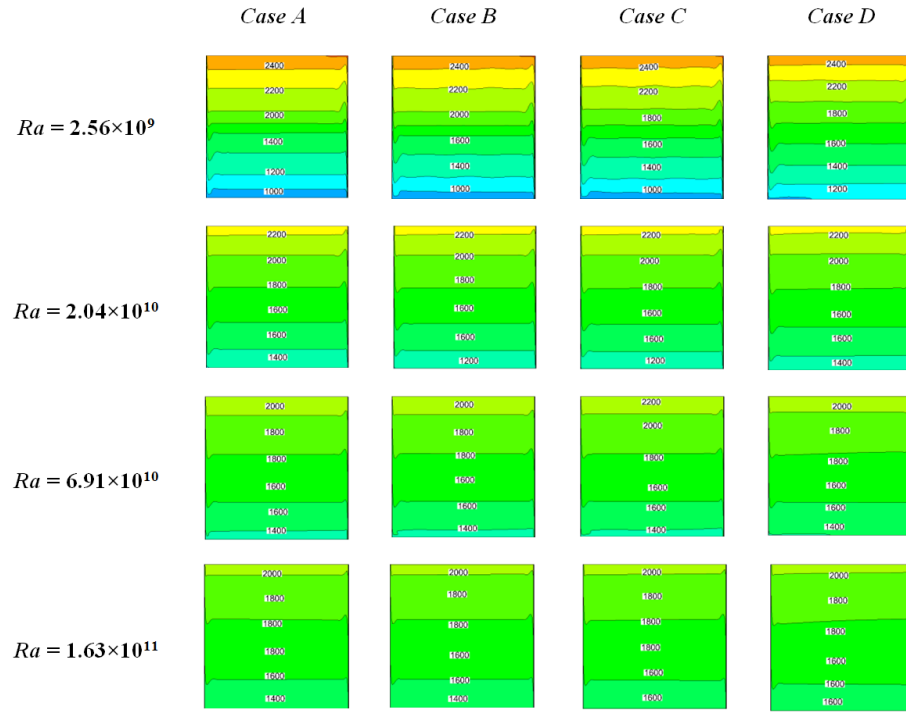
Fig. 5 Isoconcentration for all Ra numbers analysed: Case A (adobe block), Case B (red brick), Case C (concrete block) and Case D (single glass), from left to right, respectively.

Average fluid temperatures and heat fluxes from the wall to the interior of the cavity.

A quantitative comparison of the average fluid temperatures inside the cavity with different conductive walls is presented in Table 2. As we can see, average fluid temperatures for the case A are lower for all Ra numbers, decreasing by approximately 2, 4 and 10°C, regarding cases B, C and D, respectively.

Table 2. Average fluid temperatures inside the cavity.

Ra	Case A	Case B	Case C	Case D
2.56×10^9	34.1°C	36.0°C	37.9°C	46.6°C
2.04×10^{10}	35.3°C	37.3°C	39.2°C	47.1°C
6.91×10^{10}	36.1°C	38.3°C	39.9°C	47.8°C
1.63×10^{11}	37.4°C	38.9°C	40.2°C	47.9°C

The average heat fluxes of the conductive wall for a Ra= 1.63×10^{11} are graphically shown in Fig. 6. It can be seen that heat flux to the interior of the cavity is directly affected by the type of wall. The case A shows the lower heat fluxes to the interior of the cavity in agreement with indoor temperatures found previously. The case A (adobe block) decreases the energy delivery by the wall to the interior of the cavity by approximately 5, 10 and 30% regarding cases B, C and D, respectively. Concluding, the case A is the best choice in order to reach thermal comfort conditions inside the cavity. A qualitatively similar thermal behavior is observed for the rest of the Ra numbers considered in this study.

Dimensionless heat transfer

The variation of the local convective Nusselt number as function of the size of the conductive wall for Rayleigh num-

bers of 2.56×10^9 and 1.63×10^{11} are graphically shown in Fig. 7. It can be seen that for a $Ra = 2.56\times10^9$, the Nusselt number remains almost unchanged for different building materials with only slight differences at the bottom side of the wall. Furthermore, for a $Ra =1.63\times10^{11}$ is clearly observed how the Nusselt number is affected by the type of the conductive wall. From the thermal point of view, we can see again the advantage of choosing the case A respect to other conductive walls. In general, the local Nu number increases as the size of the cavity (Ra) increases.
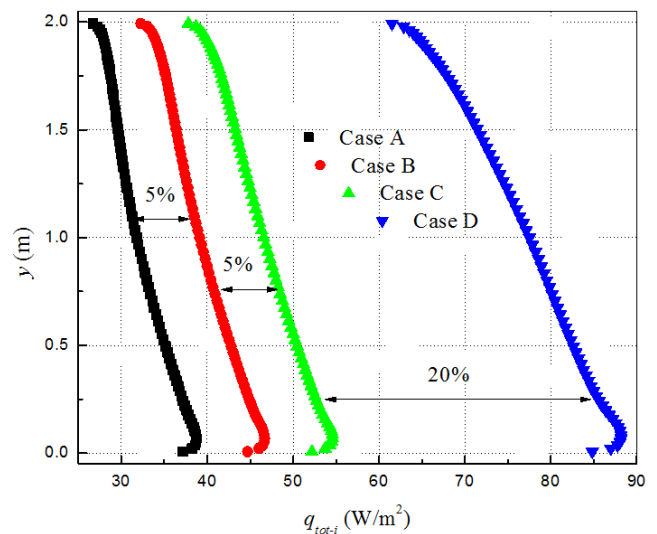

Fig. 6 Total heat fluxes to the interior of the cavity for different types of conductive walls ($Ra = 1.63\times10^{11}$).
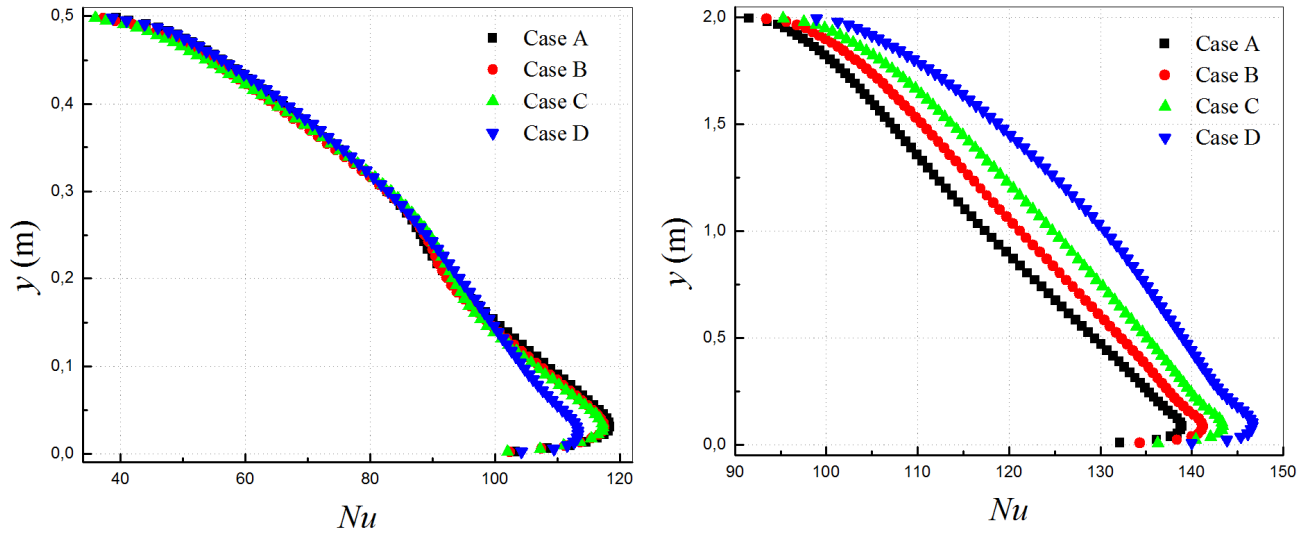
Fig. 7 Variation of local Nusselt number for the conductive wall. Cases: a) $Ra = 2.56 \times 10^9$, b) $Ra = 1.63 \times 10^{11}$.

Table 3 presents the average convective, radiative and total Nusselt number as function of the Rayleigh number in order to quantify the contribution of different conductive walls on convection, radiation and total heat transfer inside the cavity. Here, we can see that the average convection contribution is higher than radiation by 6-10% for a $Ra = 2.56 \times 10^9$, except in the case D, where radiation contribution is higher than convection by around of 3%. As it can be noted, the same behavior is observed for higher Ra numbers, presenting differences in favor of radiation contribution between 170-186%. Therefore, it is important to consider that a conjugate heat transfer analyses (convection-radiation) cannot be neglected on this type of problems. Regarding overall heat transfer intensity among cases, it is observed that differences are higher as the Ra number increases. For a highest Rayleigh number ($Ra = 1.63 \times 1011$), the case A underestimates the case B by 2.5%, followed by the case C (4.9%), and finally by the case D (13.4%).

Conclusions

In this paper, numerical calculations for the conjugate heat and mass transfer by natural convection in a square cavity filled with a mixture of Air-CO_2 are presented. The closed cavity was analyzed considering a vertical conductive wall with a high concentration of 3000 ppm and an isothermal cold wall at 25°C with a CO_2 concentration of 500 ppm; the horizontal top and bottom walls were considered adiabatic and impermeable. From the results, it can be concluded the next:

- The lowest temperature differential (ΔT) is observed for the case A for all Ra numbers.

- Thermal stratification is very different for case D at high Ra numbers compared to those found in the differentially heated square cavity problem. This behavior can be attributed to the contaminated fluid considered in this study.

- There exists a minimum difference of 200 ppm in favor of case B regarding the contaminant concentration levels for all Ra numbers.

- Average fluid temperatures for the case A are lower than cases B, C and D (2, 4 and 10°C, respectively) for all Ra numbers.

- As the Rayleigh number increases, the average fluid temperature inside the cavity increases for all cases under study.

- Higher radiation contribution is observed as the Ra number increases with maximum differences between 170-186%.

- Finally, the case A was the best choice in order to reach thermal comfort conditions at indoor spaces such as rooms.

Table 3. Average convective, radiative and total Nusselt numbers for different conductive wall materials.

Ra	Case A			Case B			Case C			Case D		
	Nu_{Conv}	Nu_{Rad}	Nu_{Tot}	Nu_{Conv}	Nu_{Rad}	Nu_{Tot}	Nu_{Conv}	Nu_{Rad}	Nu_{Tot}	Nu_{Conv}	Nu_{Rad}	Nu_{Tot}
2.56×10^9	86.3	76.5	162.8	85.5	78.2	163.7	85.4	79.9	165.3	85.6	88.3	173.9
2.04×10^{10}	109.7	157.5	267.2	108.7	161.0	269.7	108.7	164.6	273.3	107.6	180.7	288.3
6.91×10^{10}	117.7	239.1	356.8	116.4	244.2	360.6	117.8	249.7	367.5	119.0	273.8	392.8
1.63×10^{11}	117.8	319.6	437.4	120.9	327.4	448.3	123.8	335.0	458.8	128.3	367.6	495.9

Note: Average Nusselt numbers are calculated at the hot wall (conductive surface).

Acknowledgement

References

[1] D. Larson, R. Viskanta, *Transient combined laminar free convection and radiation in a rectangular enclosure*, Journal of Fluid Mechanics, 68 (1976) 65–85.

[2] B. Webb, R. Viskanta, *Radiation-induced buoyancy-driven flow in rectangular enclosures: experiment and analysis*, Journal of Heat Transfer, 109 (1987) 427–433.

[3] M. Behnia, J. Rizes, G. De Vahl Davis, *Combined radiation and natural convection in a cavity with a transparent wall and containing a non-participant fluid*. International Journal for Numerical Methods in Fluids, 10 (1990) 305–325.

[4] S. Kwon, Y. Kwon, J. Park, *Numerical study of combined natural convection and radiation in a rectangular enclosure with a transparent window on the center region of right wall*, Proceedings of 6th International Symposium on Transport Phenomena in Thermal Engineering, Seoul Korea, 1993, pp. 299–304.

[5] G. Álvarez, C. Estrada, *Numerical heat transfer in a cavity with a solar control coating deposited to a vertical semitransparent wall*, International Journal for Numerical Methods in Fluids, 34 (2000) 585–607.

[6] F.Y. Zhao, D. Liu, G.F Tang, *Conjugate heat transfer in square enclosures*, Heat Mass Transfer, 43 (2007) 907–922.

[7] J. Xamán, G. Álvarez, *Effect of heat conduction of SnS–CuxS solar control coated semitransparent wall on turbulent natural convection in a square cavity*, Numerical Heat Transfer Part A, 50 (2006),79–98.

[8] J. Xamán, J. Arce, G. Álvarez, Y. Chávez, *Laminar and turbulent natural convection combined with surface thermal radiation in a square cavity with a glass wall*. International Journal of Thermal Sciences, 47 (2008), 1630–1638.

[9] J. Xamán, G. Álvarez, J.F. Hinojosa, J.J. Flores, *Conjugate turbulent heat transfer in a cavity with a solar control coating deposited to a vertical semitransparent wall*, International Journal of Heat Fluid Flow, 30 (2009), 237-248.

[10] J. Xamán, G. Mejía, G. Álvarez, Y. Chávez, *Analysis on the heat transfer in a square cavity with a semitransparent wall: Effect of the roof materials*, International Journal of Thermal Sciences, 49 (2010), 1920-1932.

[11] G.V. Kuznetsov, M.A. Sheremet, *Conjugate heat transfer in an enclosure under the condition of internal mass transfer and in the presence of the local heat source*, International Journal of Heat and Mass Transfer, 52 (2009), 1-8.

[12] G.V. Kuznetsov, M.A. Sheremet, *Conjugate natural convection with radiation in an enclosure*, International Journal of Heat and Mass Transfer, 52 (2009), 2215-2223.

[13] G.V. Kuznetsov, M.A. Sheremet, *Numerical simulation of turbulent natural convection in a rectangular enclosure having finite thickness walls*, International Journal of Heat and Mass Transfer, 53 (2010), 163-177.

[14] G.V. Kuznetsov, M.A. Sheremet, *Conjugate natural convection in a closed domain containing a heat-releasing element with a constant heat-releasing intensity*, Journal of Applied Mechanics in Technical Physics, 51 (2010), 699-712.

[15] G.V. Kuznetsov, M.A. Sheremet, *Numerical simulation of convective heat transfer modes in a rectangular area with a heat source and conductive walls*, Journal of Heat Transfer, 132-8 (2010), 941-951.

[16] G.V. Kuznetsov, M.A. Sheremet, *Conjugate natural convection in an enclosure with a heat source of constant heat transfer rate*, International Journal of Heat and Mass Transfer, 54 (2011) 260-268.

[17] G.V. Kuznetsov, M.A. Sheremet, *A numerical simulation of double-diffusive conjugate natural convection in an enclosure*, International Journal of Thermal Sciences, 50 (2011), 1878-1886.

[18] G.V. Kuznetsov, M.A. Sheremet, *Conjugate natural convection combined with surface thermal radiation in a three dimensional enclosure with a heat source*, International Journal of Heat and Mass Transfer, 73 (2014), 340-353.

[19] M. Gijón-Rivera, J. Xamán, G. Álvarez, J. Serrano-Arellano J, *Coupling CFD-BES simulation of a glazed office with different types of windows in Mexico City*, Building and Environment, 68 (2013) 22-34.

[20] J. Serrano-Arellano, M. Gijón-Rivera, *Conjugate heat and mass transfer by natural convection in a square cavity filled with a mixture of CO_2*, International Journal of Heat and Mass Transfer, 70 (2014) 103-113.

[21] Instituto Nacional de Estadística, Geografía e Informática, (2010) *Censo de población y vivienda: Principales características de las viviendas*, retrieved April 1st, 2015 from, http://www.inegi.org.mx/.

[22] Instituto nacional de estadística e informática, (2012) *Encuesta nacional de hogares*, retrieved April 1st 2015 from, http://www.inei.gob.pe/.

[23] C. Reid, J.M. Prausnitz, B.E Poling, *The properties of gases and liquids*, Mc Graw Hill, 1987.

EDICIÓN DIGITAL

[24] R.A. Henkes, F. Van Der Vlugt, C.J. Hoogendoorn, *Natural convection flow in a square cavity calculated with low-Reynolds-number turbulence models*, International Journal of Heat and Mass Transfer, 34 (1991) 377-388.

[25] F. Modest, *Radiative Heat Transfer*, Elsevier Academic Press, New York, 2003.

[26] R. Siegel, J. Howell, *Thermal radiation heat transfer*, Taylor and Francis, New York, 1981.

[27] S. Patankar, *Numerical Heat Transfer and Fluid Flow*, Hemisphere Publishing, Washington, 1980.

[28] J. Van Doormaal, G. Raithby, *Enhancements of the SIMPLE method for predicting incompressible fluid flow,* Numerical Heat Transfer, 7 (1984) 147-163.

[29] C. Béghein, F. Haghighat, F. Allard, *Numerical study of double-diffusive natural convection in a square cavity*, International Journal of Heat and Mass Transfer 45 (1992) 883-846.

[30] R.A. Henkes, C.J. Hoogendoorn, *Comparison exercise for computations of turbulent natural convection in enclosures*, Numerical Heat Transfer, 28 (1995) 59-78.

[31] F. Ampofo, T. G. Karayiannis, *Experimental Benchmark Data for Turbulent Natural Convection in Air Filled Square Cavity*, International Journal of Heat and Mass Transfer, 46 (2003) 3551-3572.

[32] K. Velusamy, T. Sundarara, K.N. Seetharamu, *Interaction effects between surface thermal radiation and turbulent natural convection in square and rectangular enclosures*, Journal of Heat Transfer, 123 (2001) 1062-1070.

EDICIÓN DIGITAL

Marzo 2016, Vol. 5

404   Gijón-Rivera M., Serrano-Arellano J., Xamán J., Álvarez G.